Journal of Materials Chemistry A

Entrapping polysulfide by ultrathin hollow carbon sphere-functionalized separators for high-rate lithium-sulfur batteries

Journal:	*Journal of Materials Chemistry A*
Manuscript ID	TA-ART-05-2018-004800.R1
Article Type:	Paper
Date Submitted by the Author:	20-Jul-2018
Complete List of Authors:	Song, Jianjun ; Qingdao University Zhang, Chaoyue; University of Technology Sydney Guo, Xin; University of Technology Sydney, Faculty of Science ; Centre for Clean Energy Technology, University of Technology Sydney, Zhang, Jinqiang; University of Technology Sydney, Science Luo, Linqu; Qingdao University Liu, Hao; Centre for Clean Energy Technology, School of Chemistry, University of Technology, Sydney Wang, Fengyun; Qingdao University, The Cultivation Base for State Key Laboratory; Wang, Guoxiu; University of Technology Sydney, Department of Chemistry and Forensic Science

Journal Name

ARTICLE

Entrapping polysulfide by ultrathin hollow carbon sphere-functionalized separators for high-rate lithium-sulfur batteries

Received 00th January 20xx,
Accepted 00th January 20xx

DOI: 10.1039/x0xx00000x

www.rsc.org/

Jianjun Song,[ac] Chaoyue Zhang,[c] Xin Guo,[c] Jinqiang Zhang,[c] Linqu Luo,[a] Hao Liu,*[bc] Fengyun Wang*[a] and Guoxiu Wang*[c]

Lithium-sulfur batteries (LSBs) have been regarded as the most promising technology for next generation energy storage systems owing to their high energy density and low cost. However, the undesirable shuttle effect and low utilization of sulfur caused by dissolution and migration of polysulfide intermediates greatly restrict their practical application. Herein, we report a functional separator modified by novel ultrathin hollow carbon spheres (UHCS) to improve the overall performance of LSBs, and demonstrate for the first time that the nonporous hollow structured carbon materials are ideal candidates for modifying separator due to their unique property. The ultrathin and nonporous shell of the coated UHCS can act as a physical and chemical barrier to effectively entrap lithium polysulfides owing to less diffusion sites. The UHCS can also enhance the electron transfer for sulfur and accommodate the large volume change of sulfur as upper current collectors. When applying such UHCS functionalized separators, the LSBs achieved a significantly improved electrochemical performance including a high capacity of 1346.3 mAh g^{-1} at 0.2 C, and high rate capability with a discharge capacity of 458 mAh g^{-1} even at 5 C upon 1000 cycles.

Introduction

Development of advanced energy storage systems with long cycle life and high energy density is quite critical to fulfill the demand of expanding the application in all electric vehicles (EVs) and hybrid electric vehicles (HEVs). Among the various rechargeable battery devices, lithium-sulfur batteries (LSBs) are regarded as the most promising potential candidates due to their overwhelming advantages such as natural abundance, high specific energy density (2600 Wh kg^{-1}) and high theoretical capacity (1675 mAh g^{-1}).[1,2] Unfortunately, the low electrical conductivity of sulfur and the so-called "shuttle effect" originated from the diffusion of the soluble lithium polysulfides (LPSs) across the separator result in poor rate performance and severe capacity decay of batteries, greatly restricting the practical application of LSBs.[3-5]

To address these issues, plenty of researches have focused on confining sulfur into the porous host frameworks,[6] such as carbonaceous materials,[7-17] conductive polymers,[18] polar metallic oxides and nitrides.[19-31] This method has demonstrated to enhance the electrical conductivity of sulfur, and effectively restrain the shuttle effect. However, the fabrication of the designed composites always involves complex synthesis process and expensive cost of production, and thus hinders the large-scale applications of LSBs.

Recently, the modification on separators is proven to be an effective and facile strategy to depress the shuttle effect,[32-46] which involves introducing a coating layer on the cathode side of the separator. Among all candidates, carbon materials are most studied owing to their good electronic conductivity and synthetic flexibility.[47-52] The carbon coated separators can not only suppress the migration of soluble LPSs by virtue of physical and chemical effects, but also act as a second current collector to improve the conductivity of sulfur electrode, thus greatly improving the utilization of the sulfur and the cycling performance of LSBs. In order to limit the LPSs shuttling to a greater extent, most researches focus on the fabrication of porous carbonaceous materials to modify separators for enhancing the adsorption sites of LPSs.[52-60] While the porous structure also undesirably increase the diffusion sites for LPSs, and thus the shuttle effect will be severe when the adsorption cannot afford more soluble LPSs in the electrolyte at high sulfur loading, so most of the good performance is at the cost of high mass coatings on separators (usually >0.3 mg cm^{-2}), which is detrimental to the energy density of LSBs.[35] Compared with porous carbon materials, the nonporous carbon materials should theoretically possess more advantages because they have much stronger physical barrier effect, and the adsorption characteristics and good electrical conductivity are retained at same time. However, there are few reports on modifying separators using nonporous carbon materials for LSBs to date.

[a] Cultivation Base for State Key Laboratory, Qingdao University, Qingdao 266071, China. E-mail: fywang@qdu.edu.cn
[b] School of Environmental and Chemical Engineering, Shanghai University, 99 Shangda Road, Shanghai, 200444, China.
[c] Centre for Clean Energy Technology, University of Technology Sydney, Broadway, Sydney, NSW 2007, Australia. E-mail: hao.liu@uts.edu.au; Guoxiu.Wang@uts.edu.au

Electronic Supplementary Information (ESI) available: Experimental data including SEM, TEM, TG, and some electrochemical data.]. See DOI: 10.1039/x0xx00000x

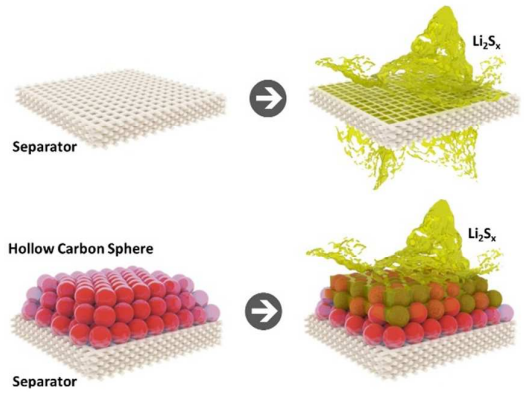

Fig. 1 Schematic configuration of shuttle effect in LSBs using PP and UHCSPP separators.

Also, the modified coating layer on the cathode side of separator can function as a "vice electrode",[61] so the soluble LPSs can be immobilized and in-situ converted into sulfur during the charge process. Considering that the hollow structure is facilitated to reserve and accommodate the large volume change for sulfur, the design of ultralight carbon materials with nonporous and hollow structure to modify separators is greatly desired for achieving excellent electrochemical performance of LSBs.

Herein, we report a functionalized separator for entrapping the soluble LPSs by coating ultrathin hollow carbon spheres (UHCS) with nonporous shell on commercial polypropylene (PP) membranes to improve the overall electrochemical performance of LSBs by simply using a carbon black/commercial sulfur composites as cathode materials. The schematic configuration of shuttle effect in LSBs using PP and UHCSPP separators is shown in Fig. 1. Generally, a porous separator is employed in conventional cells to avoid the short circuit between the cathode and anode, and benefits the fast ion transport. Unfortunately, it is also undesirably facilitated to the shuttle of soluble LPSs cross their pores, resulting in the occurrence of side reactions with lithium anode and the loss of active materials. As a contrast, the UHCS shows an ultrathin and nonporous shell with a thickness of only about 4 nm, so the stacked UHCS on the surface of separator can effectively suppress the migration of LPSs as a physical and chemical barrier layer by layer while enable the fast Li^+ transmittal. Also, they can greatly enhance the electron transfer for electrode materials and accommodate the large volume change by acting as upper current collectors. Benefit from the effective entrapping effect of LPSs and the enhanced electric conductivity, the LSBs with UHCS-functionalized separators exhibit superior cycling stability and high rate performance, delivering a high capacity of 1346.3 mAh g^{-1} at 0.2 C, and an excellent discharge capacity of 458 mAh g^{-1} even at a high rate of 5 C after 1000 cycles with a low capacity decay of 0.014 % per cycle.

Experimental

Synthesis of UHCS

The light-weight UHCS samples were synthesized by in situ carbonization of perylene-3,4,9,10-tetracarboxylic dianhydride (PTCDA) with silica spheres as templates. The silica templates (380 nm in diameter) was synthesized by a well-known Stöber method.[62] Typically, 6.6 mL of tetraethylorthosilicate (TEOS), 14 mL of ammonium hydroxide solution (25 wt%) and 25 mL of deionized water were mixed in 75 mL of ethanol. After reaction for 12 h, the uniform silica sphere can be obtained through centrifugation at 3000 rpm for 10 min. Then, the perylene-3,4,9,10-tetracarboxylic dianhydride (PTCDA) was used as carbon precursor and mixed with silica templates by a ball-milling process for 2 h. The obtained mixture was annealed at 850 °C for 4 h in argon atmosphere. During the calcination process, PTCDA could be in situ converted to ultrathin carbon layer. After etching by 5% HF solution for 24 h, the silica templates were removed, and UHCS were obtained after washing and drying at 100 °C. The synthesis route of UHCS is schematically illustrated in Fig. 2a.

For comparison, porous hollow carbon spheres (PHCS) were also prepared using glucose as carbon sources under the same preparation conditions with UCHS.

Preparation of UHCS modified polypropylene (UHCSPP) separator.

A doctor blade method was adopted to prepare UHCSPP separator. A mixture of 90 wt% UHCS and 10 wt% PVDF were dispersed in n-methylpyrrolidone (NMP) solvent to form a slurry and then uniformly pasted onto polypropylene separator (Celgard 2400). The UHCSPP separator was dried at 60 °C in a vacuum oven for 12 h. The PHCSPP separator were also prepared by coating PHCS onto polypropylene membrane under the same method.

Preparation of sulfur cathode materials.

A simple sulfur/carbon black (S/CB) composite was prepared as sulfur cathode by a conventional melt-diffusion method. Briefly, the commercial sulfur powder (Sigma-Aldrich) and carbon black (super P) were fully mixed and then kept at 155 °C for 12 h. According to thermo gravimetric analysis, the obtained S/CB composites showed 72% sulfur loading. For comparison, the S/CB composites with 57% sulfur loading are also prepared for the LSBs using the PP separator.

Preparation of Li_2S_6 solution.

The Li_2S_6 solution was synthesized through the reaction between S and Li_2S with a mole ratio of 5:1 in a mixing solvent of 1,2-dimethoxyethane/1,3-dioxolane (1:1, v/v) by stirring in an Ar-filled glovebox.

Characterizations.

The morphologies of the samples were performed on a field-emission scanning electron microscopy (FESEM, Zeiss Supra 55VP) and a transmission electron microscopy (TEM, JEOL JEM-ARM200F, at an accelerating voltage of 220 kV). Raman spectra were conducted on an inVia Renishaw Raman spectrometer system (HR Micro Raman spectrometer, Horiba JOBIN YVON US/HR800 UV) to investigate the graphitization degree of the sample. Brunauer-Emmett-Teller (BET) analyse

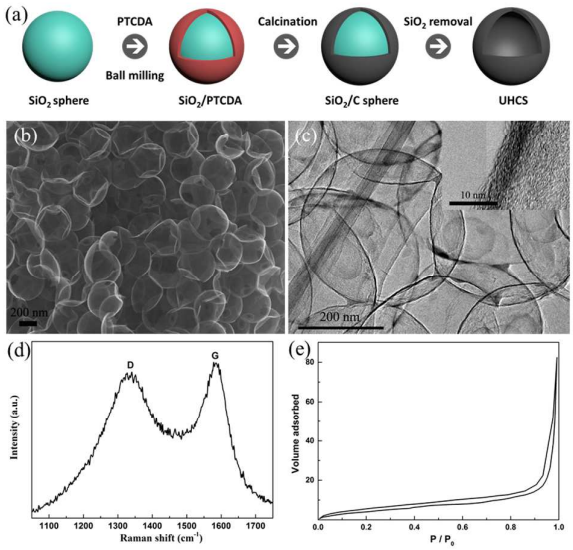

Fig. 2 Schematic illustration of the formation of UHCS (a). SEM image of UHCS samples (b). TEM image (c) and HRTEM image (inset) of UHCS samples. The Raman spectrum (d) and nitrogen adsorption/desorption isotherm (e) of UHCS

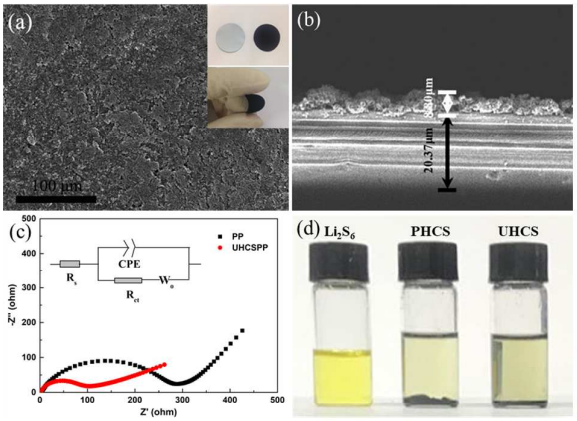

Fig. 3 (a) Low-magnification surface SEM image and the digital image (inset) of the UHCSPP separator. (b) Cross-sectional SEM image of the UHCSPP separator. (c) EIS curves and equivalent circuit (inset) of fresh LSBs using PP and UHCSPP separators. (d) Photograph of sealed vials of a Li_2S_6/DME/DOL solution soaking with PHCS and UHCS in glovebox for 2 h, respectively.

was applied to determine the surface area at a relative pressure of P/P_0 = 0.05-0.25. TGA analysis was used to analyse the sulfur contents of S/CB composites on a TA Instruments (SDT 2960) under N_2 atmosphere from room temperature to 600 °C with a heating rate of 10 °C min^{-1}. X-ray photoelectron spectroscopy (XPS) measurements were performed on an ESCALAB250Xi (Thermo Scientific, UK) equipped with mono-chromated Al Kα (energy 1486.68 eV).

Electrochemical measurements

The sulfur electrodes were prepared by mixing the S/CB, carbon black (super P), and poly(vinylidene fluoride) (PVDF) with a mass ratio of 8:1:1 in N-methyl-2-pyrrolidone (NMP) solvent to form a slurry. The slurry was pasted onto aluminium foil and dried in a vacuum oven at 60 °C for 12 h. The sulfur mass loading in working electrodes is about 1.2-1.5 mg cm^{-2}. The electrolyte is prepared with 1 M lithium bis(trifluoromethane sulfonimide) (LiTFSI) in a mixing solvent of DME/DOL (1:1, v/v) with 0.1 M $LiNO_3$. The electrolyte amount in coin cell was about 40 μL, and the Coin-type (CR2032) cells were used and assembled in an Ar-filled glovebox, in which H_2O and O_2 contents were less than 0.1 ppm. The galvanostatic discharge/charge performance of LSBs were tested on a LAND CT2001A testing system over a potential range of 1.7-2.8 V. Electrochemical impedance spectroscopy (EIS) tests were performed on an electrochemical workstation (CHI 660E) from 100 kHz to 10 mHz with an applied amplitude of 5 mV.

Results and discussion

The morphology of the prepared UHCS is investigated by scanning electron microscopy (SEM) and transmission electron microscopy (TEM). As is shown in Fig. 2b and Fig. S1a, the samples show large-scale uniform well-dispersed hollow spheres morphology, which is obviously different from the bulk morphology of agglomerated PHCS synthesized with glucose (Fig. S2). Some of UHCS possess large holes caused by removal of silica templates, and it will be beneficial to store the entrapped LPSs and accommodate the large volume change during cycling. The diameter of UHCS samples is about 380 nm, which is similar to SiO_2 sphere templates and SiO_2/C (Fig. S3). The TEM images (Fig. 3c and Fig. S1b) confirm the hollow sphere structure of UHCS inherited from the silica templates, and also demonstrate their uniform ultrathin shell thickness of only about 4 nm, which can greatly decrease the weight of modified separator. No obvious pores on the shell of spheres can be found from the HRTEM image (inset of Fig. 2c).

Raman spectrum of UHCS samples in Fig. 2d shows intense D (disordered) band and G (graphitic) band. The peak area ratio of D band to G band (A_D/A_G) can be used as an estimation of the graphitization degree. The UHCS samples clearly exhibit a lower value of A_D/A_G than that of the carbon synthesized with glucose (Fig. S4), illuminating their better graphitization degree, which can be ascribed to the naphthalene rings-structured PTCDA. The good graphitization degree is facilitated to trap polysufides and contribute to the electronic conductivity for electrode materials.[63,64] The nitrogen sorption test was performed to investigate the pore information of UHCS. The BET results in Fig. 3d reveal that the UHCS has a surface area of only 10 m^2 g^{-1} and a small pore volume of 0.12 cm^3 g^{-1}, which is consistent with HRTEM analysis, illustrating an almost nonporous characteristic of UHCS. The formation of nonporous structure can be ascribed to the high carbon content in the molecule of PTCDA ($C_{24}H_8O_6$) and the ultrathin shell. A small amount of gas produced during heat treatment can easily release along the shell, and thus PTCDA are in-situ converted into an ultrathin nonporous structured carbon layer. As a contrast, the glucose easily agglomerated and formed a bulk during heat

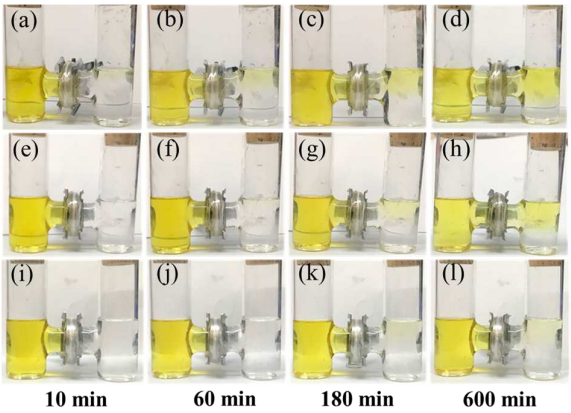

Fig. 4. Diffusion test of polysulfides with pristine PP separator (a-d), PHCSPP separator (e-h) and UHCSPP separator (i-l).

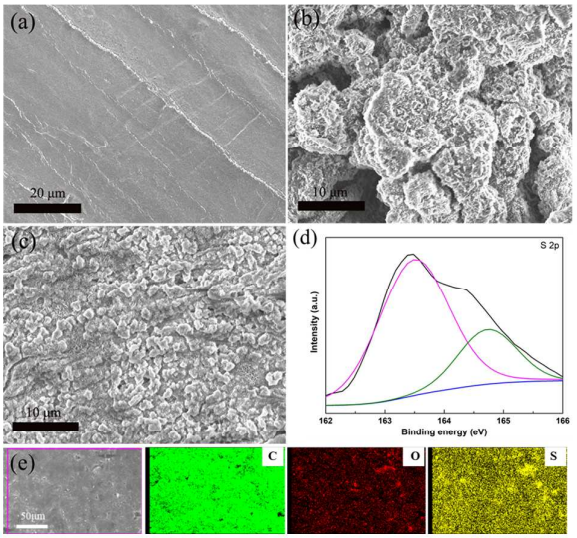

Fig. 5 Typical SEM images of pristine lithium (a) and the cycled metallic lithium of the LSBs using PP (b) and UHCSPP (c) separators. (d) High-resolution S 2p XPS spectra of the cycled UHCSPP separator. (e) SEM image and corresponding EDX elemental mapping of the cycled UHCSPP separator.

treatment, so the formation of large amounts of gas created a porous structure. As shown in Fig. S5, the PHCS possess large surface area of 531 m^2 g^{-1} and pore volume of 0.34 cm^3 g^{-1}. Compared with porous materials when modifying separator, the UHCS have more advantages to suppress the shuttle of LPSs as physical barrier due to the less diffusion sites.

Fig. 3a shows the surface morphology and flexibility (inset) of UHCSPP separator. The coating UHCS shows a dense layer with uniform distribution on the surface. After the facile coating of UHCS slurry, the designed modified separator exhibits good flexibility. In favor of the ultrathin hollow structure, the coating thickness and the mass loading are 8.8 μm (Fig. 3b) and 0.2 mg cm^{-2}, respectively. The electrochemical impedance spectroscopy (EIS) of fresh LSBs with PP and UHCSPP separators were employed to evaluate the effect of UHCSPP separator on internal resistance (Fig. 3c). Nyquist profiles of both cells present a quasi-semicircle at the moderate frequency region and a sloping line at the low frequency region, which are relevant to a charge transfer process and a Warburg diffusion process, respectively. The charge transfer resistance (R_{ct}) in the cell with UHCSPP separator show a much lower value than that of cell with PP separator. The results clearly prove that the coated UHCS can remarkably decrease the resistance of the electrode owing to its high electronic conductivity.

To check the absorption ability of UHCS and PHCS to LPSs, the Li_2S_6 adsorption test was conducted by soaking 20 mg UHCS into 2 mM Li_2S_6 solution within a sealed vial, and all operations were performed in an Ar-filled glovebox. As shown in Fig. 3d, the solution colors in both samples clearly change from yellow to dilute yellow after mixing for 2 h, demonstrating their absorption ability to LPSs. And the PHCS shows slightly lighter colors owing to their more adsorption sites of porous structure.

Diffusion test of polysulfides in 2 mM Li_2S_6 solution with pristine PP, PHCSPP and UHCSPP separators were performed to show the comprehensive effect of physical barrier and absorption ability, as shown in Fig. 4. With the increase of time, the polysulfides show fast diffusion across the pristine PP separator. By contrast, the colors of the right glass tube are lighter than that of pristine PP separator at each time when applied a PHCSPP separator. However, the diffusion is still severe when time goes long (Fig. 4h). After using the UHCSPP separator, the polysulfides diffusion are strongly inhibited even after 600 min, demonstrating the strong trapping effect of UHCS. The stacked nonporous UHCS can effectively restrain the polysulfides layer by layer, and thus enhance the utilization of sulfur and prolong the cycle life of cells.

To further verify the trapping ability of UHCSPP separator, the cycled lithium anode and separator were investigated. The LSBs with PP and UHCSPP separators were galvanostatically discharged and charged at 1 C for 100 cycles and then disassembled in a glove box. Fig. 5 shows the SEM images of the fresh lithium and cycled lithium anode. A smooth and flat morphology can be found on the surface of fresh lithium metal. While the rugged surface with severe corrosion is found on the cycled lithium anode with PP separator, which can be resulted from the deposition of Li_2S_2/Li_2S reacted between the migrated LPSs and lithium metal during the cycling.[58] Obviously, the lithium anode cycled with UHCSPP separator possesses a relatively smooth and uniform surface (Fig. 5c). X-ray photo-electron spectroscopy (XPS) measurement of cycled UHCSPP separator was performed and a pair of peaks at 164.7 and 163.5 eV are observed at S 2p region, indicating the elemental sulfur (S_8) entrapped within UHCS layer (Fig. 5d). SEM image and corresponding energy-dispersive X-ray spectroscopy (EDX) elemental mapping (Fig. 5e) of cycled UHCSPP separator further confirm the distribution of elemental carbon and sulfur. The results fully demonstrate that the soluble LPSs can be effectively entrapped and re-utilized through the functional barrier of the UHCS layer.

The electrochemical performance of LSBs with PP and UHCSPP separators was tested to investigate the effect of UHCS modified separator. The simple CB/S composites with 72 wt% S content (Fig. S6a) were prepared and used as sulfur cathode materials for LSBs with PHCSPP and UHCSPP separators. To make the sulfur ratio

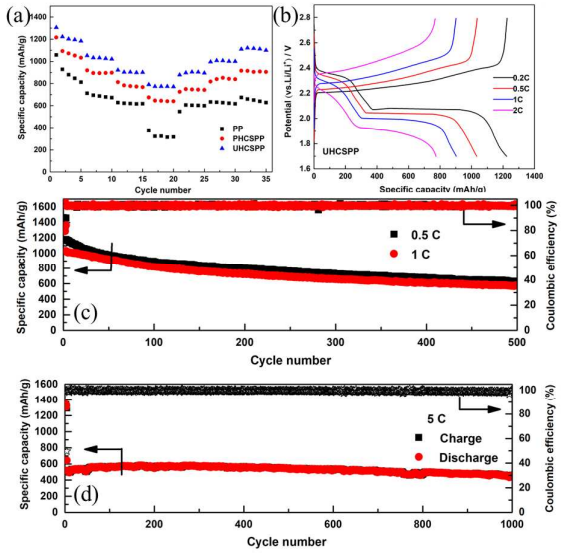

Fig. 6 (a) Rate performance of LSBs using PP, PHCSPP, and UHCSPP separators, respectively. (b) First charge/discharge curves of LSBs using UHCSPP separators at various rates. (c) Long-term cycling performance of LSBs with UHCSPP separators at rates of 0.5 C and 1 C, respectively. (d) Long-term cycling performance of LSBs with UHCSPP separators at a high rate of 5 C.

comparable, the CB/S composites with 57 wt% S content (Fig. S6b) were used for testing in the LSBs with PP separators.

The rate performance of LSBs with PP, PHCSPP and UHCSPP separators were performed by discharging and charging from 0.2 C to 2 C stepwise, and then switched back to 0.2 C (Fig. 6a). The LSBs with PHCSPP and UHCSPP separators show high initial discharge capacities of 1216 and 1305 mAh g^{-1} at 0.2 C, respectively. These values are much higher than that of pristine PP separators (1058 mAh g^{-1}), which can be attributed to the better electron transfer and trapping effect of discharging LPSs intermediates. The LSBs with UHCSPP separators exhibit superior discharge capacities of 1052, 921 and 790 mAh g^{-1} at 0.5, 1 and 2 C, respectively, which are higher than those of LSBs with PHCSPP separators (919, 813 and 675 mAh g^{-1} at 0.5, 1 and 2 C, respectively). This enhancement can be ascribed to the better inhibition to LPSs diffusion. As a contrast, with the increasing of current density, the electrochemical performance of LSBs with PP separators show a sharp decrease with discharge capacities of 712, 628 and 375 mAh g^{-1} at 0.5, 1 and 2 C, respectively. After switching the current densities back to 0.5 C and 0.2 C, the LSBs with UHCSPP separators show high reversible capacities of 996 and 1110 mAh g^{-1} (94.6% and 85% of the original discharge capacities), respectively, reflecting its stable and reversible characteristics by using the UHCS functionalized separators. While the capacities of the cells using PP separators present worse reversible capacities of only 634 and 674 mAh g^{-1}, corresponding to the 89% and 63.7% of the original discharge capacities. Clearly, the results prove that UHCS functionalized separator can remarkably improve the rate capability of LSBs owing to their strong trapping effect to LPSs.

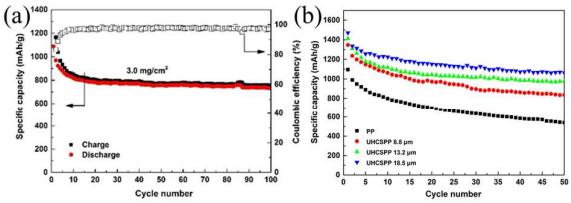

Fig. 7 (a) Cycling performance of LSBs using UHCSPP separators with a high sulfur loading of 3 mg cm^{-2} at 0.2 C. (b) Cycling performance of LSBs using PP separators and UHCSPP separators with different coating thicknesses at 0.2 C.

The charge/discharge curves in different rates for the cells with UHCSPP separator are shown in Fig. 6b. Each discharge curve shows two typical discharge potential plateaus. The upper discharge voltage plateau around 2.3 V stands for the conversion of sulfur to high-order LPSs (Li_2S_{4-8}). The lower discharge plateau around 2.1 V is related to their further reduction to Li_2S_2/Li_2S.[65] The two continuous plateaus in charge curves at 2.2 and 2.4 V indicate the oxidation reactions of Li_2S_2/Li_2S to Li_2S_8/S_8 during the charging processes. The charge/discharge curves of the LSBs with UHCSPP separators at various rates show more flat and stable plateaus compared to the cells with PP separators (Fig. S7). The cells with UHCSPP separators also show lower voltage plateau gaps between the charge/discharge curves than the cells with PP separators, especially at high rate, confirming their lower polarization and better reversibility.

Fig. 6c shows the cycling performance of the cells using UHCSPP separators at 0.5 and 1 C for 500 cycles. The cells show superior cycling performance with discharge capacities of 632 and 575 mAh g^{-1} at 0.5 C and 1 C after cycling 500 cycles, which are much higher than the cells with PP and PHCSPP separators (Fig. S8). In addition, high Columbic efficiency of almost 100 % can be obtained. The long-term cycling performance at high rate of LSBs using UHCSPP separators is also investigated and shown in Fig. 6d. The cell exhibits excellent cycling stability with an initial discharge capacity of 643 mAh g^{-1}, and a high discharge capacity 458 mAh g^{-1} after 1000 cycles at a high rate of 5 C, and the capacity decay is only 0.014 % per cycle, confirming the remarkable improvement of UHCSPP separators on high rate performance of LSBs.

The cycling performance of the cells using UHCSPP separators with high sulfur loading of 3.0 mg cm^{-2} is conducted at 0.2 C, shown in Fig. 7a. The cells show good electrochemical performances with an initial discharge capacity of 1087 mAh g^{-1} and a high discharge capacity of 730 mAh g^{-1} at 0.2 C after 100 cycles, and the performance almost keep stable after the preliminary decay at first 20 cycles, which can be also proved by the charge/discharge curves at different cycles (Fig. S9). Obviously, the results demonstrate that the UHCSPP separator can effectively enhance the performance of LSBs at a high sulfur loading.

To investigate the coating thickness effect on electrochemical performance, the UHCSPP with different coating thicknesses of 13.2 and 18.5 μm (SEM images in Fig. S10) were also prepared, and the coating mass are 0.3 mg cm^{-2} and 0.45 mg cm^{-2}, respectively. The cycling performance of LSBs using pristine PP separator and UHCSPP separators with different coating thicknesses (8.8, 13.2 and

18.5 μm) at 0.2 C are shown in Fig. 7b. The cell with PP separator exhibits initial discharge capacity of 1095.4 mAh g^{-1}. After cycling for 50 cycles, the cell with PP separator shows a low capacity retention of 49.3% and a low discharge capacity of only 540 mAh g^{-1}. All the LSBs using UHCSPP separators show higher discharge capacities and better cycling performance than that of LSBs using PP separator. With the increase of coating thickness, the electrochemical performance become more stable, demonstrating the effective trapping of UHCS layer to LPSs. Particularly, LSBs using UHCSPP separator with thickness of 18.5 μm exhibit admirable performance with initial discharge capacity of 1471.9 mAh g^{-1} and high reversible capacity of 1063.7 mAh g^{-1} after 50 cycles (capacity retention of 72.3%).

The superior electrochemical performances with excellent rate capability and cycling stability can be attributed to the design of UHCS functionalized separator, which shows much better performance with less coating mass than most of the previously reported carbon-based modified separators,[50-54,57-60,66-67] as summarized in Table S1. Firstly, the light-weight property can greatly decrease the weight of coating layer owing to their ultrathin shell and hollow structure, benefiting the high energy density of LSBs. Secondly, the stacked UHCS with nonporous property can effectively obstruct and adsorb the migrating soluble LPSs layer by layer via both physisorption and chemisorption, and thus reduce the occurrence of side reactions. Thirdly, the hollow structure of UHCS can store the absorbed active materials and accommodate the large volume change, so enhance the re-utilization of sulfur. Meanwhile, the UHCS layer with good electrical conductivity on separator can decrease the internal resistance of a cell by acting as a second current collector,[68] greatly improving the redox kinetics.

Conclusions

Novel ultrathin hollow carbon spheres are employed to modify the commercial polypropylene separators in lithium-sulfur batteries. With this functionalized separator, the LSBs exhibit excellent rate capability and cycling stability. The coated hollow carbon spheres with ultrathin nonporous structure can remarkably entrap soluble LPSs as a physical and chemical barrier and reduce the internal resistance of cells. Therefore, the nonporous carbonaceous materials with hollow structure are highly desired to enhance the electrochemical performance and speed up the commercialization of LSBs by modifying separator.

Conflicts of interest

There are no conflicts to declare.

Acknowledgements

This work was financially supported by the Australian Renewable Energy/Agency (ARENA) project (ARENA 2014/RND106) and Australian Research Council Discovery Project (DP180102297). J. Song is grateful for the China Postdoctoral Science Foundation Funded Project (2018M630747). C. Zhang acknowledges the financial support of the China Scholarship Council (CSC).

Notes and references

1 D. Peramunage and S. Licht, *Science*, 1993, **261**, 1029-1032.
2 X. Ji, K. T. Lee and L. F. Nazar, *Nature Materials*, 2009, **8**, 500.
3 S. Lu, Y. Cheng, X. Wu and J. Liu, *Nano Letters*, 2013, **13**, 2485-2489.
4 H. Wang, Y. Yang, Y. Liang, J. T. Robinson, Y. Li, A. Jackson, Y. Cui and H. Dai, *Nano Letters*, 2011, **11**, 2644-2647.
5 Y. Qiu, W. Li, W. Zhao, G. Li, Y. Hou, M. Liu, L. Zhou, F. Ye, H. Li, Z. Wei, S. Yang, W. Duan, Y. Ye, J. Guo and Y. Zhang, *Nano Letters*, 2014, **14**, 4821-4827.
6 S. Rehman, K. Khan, Y. Zhao and Y. Hou, *Journal of Materials Chemistry A*, 2017, **5**, 3014-3038.
7 L. Kong, B. Li, H. Peng, R. Zhang, J. Xie, J. Huang and Q. Zhang, *Advanced Energy Materials*, 2018, 1800849.
8 J. Liu, T. Yang, D.-W. Wang, G. Q. Lu, D. Zhao and S. Z. Qiao, *Nature Communications*, 2013, **4**, 2798.
9 S. Feng, J. Song, S. Fu, C. Zhu, Q. Shi, M.-K. Song, D. Du and Y. Lin, *Journal of Materials Chemistry A*, 2017, **5**, 23737-23743.
10 H. Wu, L. Xia, J. Ren, Q. Zheng, C. Xu and D. Lin, *Journal of Materials Chemistry A*, 2017, **5**, 20458-20472.
11 J. Liang, Z.-H. Sun, F. Li and H.-M. Cheng, *Energy Storage Materials*, 2016, **2**, 76-106.
12 J. Song, Z. Yu, M. L. Gordin and D. Wang, *Nano Letters*, 2016, **16**, 864-870.
13 W. Yang, W. Yang, A. Song, G. Sun and G. Shao, *Nanoscale*, 2018, **10**, 816-824.
14 D. Xiao, Q. Li, H. Zhang, Y. Ma, C. Lu, C. Chen, Y. Liu and S. Yuan, *Journal of Materials Chemistry A*, 2017, **5**, 24901-24908.
15 H. Zhang, Z. Zhao, Y.-N. Hou, Y. Tang, Y. Dong, S. Wang, X. Hu, Z. Zhang, X. Wang and J. Qiu, *Journal of Materials Chemistry A*, 2018, **6**, 7133-7141.
16 M. Li, Y. Zhang, F. Hassan, W. Ahn, X. Wang, W. W. Liu, G. Jiang and Z. Chen, *Journal of Materials Chemistry A*, 2017, **5**, 21435-21441.
17 G. Hao, C. Tang, E. Zhang, P. Zhai, J. Yin, W. Zhu, Q. Zhang and S. Kaskel, *Advanced Materials*, 2017, **29**, 1702829.
18 W. Li, Q. Zhang, G. Zheng, Z. W. Seh, H. Yao and Y. Cui, *Nano Letters*, 2013, **13**, 5534-5540.
19 S. Rehman, T. Tang, Z. Ali, X. Huang and Y. Hou, Small, 2017, **20**, 1700087.
20 Z. Wei Seh, W. Li, J. J. Cha, G. Zheng, Y. Yang, M. T. McDowell, P.-C. Hsu and Y. Cui, *Nature Communications*, 2013, **4**, 1331.
21 C. J. Hart, M. Cuisinier, X. Liang, D. Kundu, A. Garsuch and L. F. Nazar, *Chemical Communications*, 2015, **51**, 2308-2311.
22 X. Liang, C. Hart, Q. Pang, A. Garsuch, T. Weiss and L. F. Nazar, *Nature Communications*, 2015, **6**, 5682.
23 Z. Sun, J. Zhang, L. Yin, G. Hu, R. Fang, H.-M. Cheng and F. Li, *Nature Communications*, 2017, **8**, 14627.
24 D.-R. Deng, F. Xue, Y.-J. Jia, J.-C. Ye, C.-D. Bai, M.-S. Zheng and Q.-F. Dong, *ACS Nano*, 2017, **11**, 6031-6039.
25 Z. Li, B. Y. Guan, J. Zhang and X. W. Lou, *Joule*, 2017, **1**, 576-587.
26 M. Fang, Z. Chen, Y. Liu, J. Quan, C. Yang, L. Zhu, Q. Xu and Q. Xu, *Journal of Materials Chemistry A*, 2018, **6**, 1630-1638.
27 J. Xu, W. Zhang, Y. Chen, H. Fan, D. Su and G. Wang, *Journal of Materials Chemistry A*, 2018, **6**, 2797-2807.
28 M. Wang, L. Fan, X. Wu, D. Tian, J. Cheng, Y. Qiu, H. Wu, B. Guan, N. Zhang, K. Sun and Y. Wang, *Journal of Materials Chemistry A*, 2017, **5**, 19613-19618.

29 D.-R. Deng, J. Lei, F. Xue, C.-D. Bai, X.-D. Lin, J.-C. Ye, M.-S. Zheng and Q.-F. Dong, *Journal of Materials Chemistry A*, 2017, **5**, 23497-23505.
30 L. Luo, S.-H. Chung and A. Manthiram, *Journal of Materials Chemistry A*, 2018, **6**, 7659-7667.
31 L. Kong, X. Chen, B. Li, H. Peng, J. Huang, J. Xie and Q. Zhang, *Advanced Materials*, 2018, **30**, 1705219.
32 L. Luo, X. Qin, J. Wu, G. Liang, Q. Li, M. Liu, F. Kang, G. Chen and B. Li, *Journal of Materials Chemistry A*, 2018, DOI: 10.1039/C8TA01726C.
33 J. Wang, J. Liang, J. Wu, C. Xuan, Z. Wu, X. Guo, C. Lai, Y. Zhu and D. Wang, *Journal of Materials Chemistry A*, 2018, **6**, 6503-6509.
34 M. Li, C. Wang, L. Miao, J. Xiang, T. Wang, K. Yuan, J. Chen and Y. Huang, *Journal of Materials Chemistry A*, 2018, **6**, 5862-5869.
35 F. Pei, L. Lin, A. Fu, S. Mo, D. Ou, X. Fang and N. Zheng, *Joule*, 2018, **2**, 323-336.
36 J. Song, D. Su, X. Xie, X. Guo, W. Bao, G. Shao and G. Wang, *ACS Applied Materials & Interfaces*, 2016, **8**, 29427-29433.
37 L. Zhang, F. Wan, X. Wang, H. Cao, X. Dai, Z. Niu, Y. Wang and J. Chen, *ACS Applied Materials & Interfaces*, 2018, **10**, 5594-5602.
38 L. Tan, X. Li, Z. Wang, H. Guo and J. Wang, *ACS Applied Materials & Interfaces*, 2018, **10**, 3707-3713.
39 K. Wu, Y. Hu, Z. Shen, R. Chen, X. He, Z. Cheng and P. Pan, *Journal of Materials Chemistry A*, 2018, **6**, 2693-2699.
40 Y. C. Jeong, J. H. Kim, S. H. Kwon, J. Y. Oh, J. Park, Y. Jung, S. G. Lee, S. J. Yang and C. R. Park, *Journal of Materials Chemistry A*, 2017, **5**, 23909-23918.
41 X. Song, S. Wang, G. Chen, T. Gao, Y. Bao, L.-X. Ding and H. Wang, *Chemical Engineering Journal*, 2018, **333**, 564-571.
42 L. Shi, F. Zeng, X. Cheng, K. H. Lam, W. Wang, A. Wang, Z. Jin, F. Wu and Y. Yang, *Chemical Engineering Journal*, 2018, **334**, 305-312.
43 Y. Lai, P. Wang, F. Qin, M. Xu, J. Li, K. Zhang and Z. Zhang, *Energy Storage Materials*, 2017, **9**, 179-187.
44 S. Bai, X. Liu, K. Zhu, S. Wu and H. Zhou, *Nature Energy*, 2016, **1**, 16094.
45 Z. Cheng, H. Pan, Z. Xiao, D. Chen, X. Li and R. Wang, *Journal of Materials Chemistry A*, 2018, DOI: 10.1039/C8TA01298A.
46 Z. Zhang, G. Wang, Y. Lai, J. Li, Z. Zhang and W. Chen, *Journal of Power Sources*, 2015, **300**, 157-163.
47 Z. Du, C. Guo, L. Wang, A. Hu, S. Jin, T. Zhang, H. Jin, Z. Qi, S. Xin, X. Kong, Y.-G. Guo, H. Ji and L.-J. Wan, *ACS Applied Materials & Interfaces*, 2017, **9**, 43696-43703.
48 P. Han and A. Manthiram, *Journal of Power Sources*, 2017, **369**, 87-94.
49 L. Zhu, L. You, P. Zhu, X. Shen, L. Yang and K. Xiao, *ACS Sustainable Chemistry & Engineering*, 2018, **6**, 248-257.
50 R. Ponraj, A. G. Kannan, J. H. Ahn, J. H. Lee, J. Kang, B. Han and D.-W. Kim, *ACS Applied Materials & Interfaces*, 2017, **9**, 38445-38454.
51 X. Gu, C.-j. Tong, C. Lai, J. Qiu, X. Huang, W. Yang, B. Wen, L.-m. Liu, Y. Hou and S. Zhang, *Journal of Materials Chemistry A*, 2015, **3**, 16670-16678.
52 H. Shao, F. Ai, W. Wang, H. Zhang, A. Wang, W. Feng and Y. Huang, *Journal of Materials Chemistry A*, 2017, **5**, 19892-19900.
53 Z. Zhang, G. Wang, Y. Lai, J. Li, Z. Zhang and W. Chen, *Journal of Power Sources*, 2015, **300**, 157-163.
54 J. Balach, T. Jaumann, M. Klose, S. Oswald, J. Eckert and L. Giebeler, *Advanced Functional Materials*, 2015, **25**, 5285-5291.
55 J.-Q. Huang, W. G. Chong, Q. Zheng, Z.-L. Xu, J. Cui, S. Yao, C. Wang and J.-K. Kim, *Electrochimica Acta*, 2018, **268**, 1-9.
56 R. K. Selvan, P. Zhu, C. Yan, J. Zhu, M. Dirican, A. Shanmugavani, Y. S. Lee and X. Zhang, *Journal of Colloid and Interface Science*, 2018, **513**, 231-239
57 S.-H. Chung and A. Manthiram, *Advanced Functional Materials*, 2014, **24**, 5299-5306.
58 J. Zhu, Y. Ge, D. Kim, Y. Lu, C. Chen, M. Jiang and X. Zhang, *Nano Energy*, 2016, **20**, 176-184.
59 H. J. Peng, Z. W. Zhang, J. Q. Huang, G. Zhang, J. Xie, W. T. Xu, J. L. Shi, X. Chen, X. B. Cheng and Q. Zhang, *Advanced Materials*, 2016, **28**, 9551-9558.
60 G. Zhou, L. Li, D. W. Wang, X. Y. Shan, S. Pei, F. Li and H. M. Cheng, *Advanced Materials*, 2015, **27**, 641-647.
61 Y. Hao, D. Xiong, W. Liu, L. Fan, D. Li and X. Li, *ACS Applied Materials & Interfaces*, 2017, **9**, 40273-40280.
62 W. Stöber, A. Fink and E. Bohn, *Journal of Colloid and Interface Science*, 1968, **26**, 62-69.
63 C.-H. Chang, S.-H. Chung and A. Manthiram, *Journal of Materials Chemistry A*, 2015, **3**, 18829-18834.
64 H. Liu, W. Li, D. Shen, D. Zhao and G. Wang, *Journal of the American Chemical Society*, 2015, **137**, 13161-13166.
65 G. Zheng, Y. Yang, J. J. Cha, S. S. Hong and Y. Cui, *Nano Letters*, 2011, **11**, 4462-4467.
66 U. Stoeck, J. Balach, M. Klose, D. Wadewitz, E. Ahrens, J. Eckert and L. Giebeler, *Journal of Power Sources*, 2016, **309**, 76-81.
67 P.-Y. Zhai, H.-J. Peng, X.-B. Cheng, L. Zhu, J.-Q. Huang, W. Zhu and Q. Zhang, *Energy Storage Materials*, 2017, **7**, 56-63.
68 Y.-S. Su and A. Manthiram, *Nature Communications*, 2012, **3**, 1166.

TOC

Novel ultrathin hollow carbon spheres with nonporous shell are employed as polysulfide reservoir to improve overall performance of Li-S batteries.